INTER-CALIBRATION OF PASSIVE MICROWAVE BRIGHTNESS TEMPERATURE OBSERVED BY FY-3B/MWRI AND AQUA/AMSR-E ON ARCTIC

*Haihua Chen, Xiaotong Tang, Lele Li, Lei Guan**

Department of Marine Technologies, College of Information Science and Engineering, Ocean University of China, Qingdao, 266100

ABSTRACT

The inter-calibration of the brightness temperature between FY-3B/MWRI and Aqua/AMSR-E is studied by 8858 files of MWRI L1 and 9327 files of AMSR-E L2A from November 18, 2010 to September 30, 2011 with the spatial coverage on north of 60°N. According to the polar projection, time-space matching and linear fitting, the inter-calibration parameters of the MWRI and AMSR-E are achieved. From the scatters of each channel and the statistic analysis, it shows that there are some deviation between the two sensors but it has obvious consistency on overall trend and the correlation coefficients of the TB in H and V polarization among all channel are more than 0.9. Using the linear regression analysis, the slopes and intercepts of the fitting equations for 10.7~89.0GHz H/V ascending and descending TB data on every month of the data sets were achieved. After inter-calibration the statistic parameters between the two sensors are obviously optimized.

Index Terms — Microwave Radiation Imager (MWRI); FY-3B; AMSR-E; brightness temperature; inter-calibration

1. INTRODUCTION

Arctic is an important part of the global climate system. Recent years the sea ice on arctic has been changing rapidly, especially in summer the sea ice is decreasing significantly [1]. The passive microwave remote sensing has been widely used in arctic research because of its all-weather and all-day detection ability[2]. At present, Space-borne Microwave Radiometers mainly include the SMMR on Nimbus-7[3] , the DMSP series of SSM/I [4], the TMI of the TRMM, and AMSR-E on NASA Aqua satellite launched in May 2002 which are used to obtain the land, sea, sea ice and snow cover parameters[2,5], and observe atmospheric water and energy cycle changes. Comparing with SMMR, SSM/I and other microwave sensors, AMSR-E has advantages of multiple channels, widely frequency range and high resolution. The National Snow and Ice Center (NSIDC) received the AMSR-E data, and had released different level products about the Polar Regions. On October 4, 2011, the instrument failure occurred in AMSR-E sensor and the new sensor AMSR2 following the Mission of AMSR-E, was carried on the SHIZUKU satellite of GCOM (Global Change Observation Mission) on May 18, 2012. The Microwave Radiation Imager (MWRI) on board the FY-3B satellite of China Meteorological Administration were launched on November 5, 2010, which can provide new passive microwave data to related research.

The instrument's designs of the space-borne passive microwave sensors are difference in frequency band, calibration system, observation time and angle of the incidence which will lead to the deviation among the sensor's data. Through the inter-calibration to evaluate the data quality, correct data deviation, eliminate data inconsistency, researchers can obtain long-term continuous observation data which is important to study the earth's environment change, weather forecasting and climate changing. Researchers have studied the inter-calibration between the SSM/I, SMMR and SSM/I [6], Arata Okuyama et al. calibrated AMSR2 with TMI and AMSR-E respectively[7], Imaoka K et al. carried out data comparison and calibration analysis for AMSR-E and AMSR2[8], Hu Tongxi et al. compared the slow mode L1S in the AMSR-E with the land surface observation data of AMSR2 and established the linear model of the two sensors[9], Jinyang Du based on the correction method of Double-Difference, took MWRI as the reference target and cross-calibrated AMSR-E and AMSR2[10]. Huang Wei compared the MWRI and AMSR-E brightness temperature data in the bohai and yellow sea area of China[11], Wang Gongxue et al. calibrated the FY-3B/MWRI and FY-3C /MWRI in Greenland[12]. Satellite FY-3 series will be used 15 years and the long time series of data will be provided for land water cycle and climate change research[13]. The inter-calibration of the MWRI and AMSR-E brightness temperature is helpful to not only the improvement of passive microwave sensors, but also the research of the ice and snow monitoring on Arctic and global climate change.

In this paper, the inter-calibration of the brightness temperature from 10.7GHz to 89.0GHz between MWRI and AMSR-E is studied on Arctic with statistical inter-calibration approach. The inter-calibration parameters and evaluation are achieved. This paper is organized as follows. In section 2, the data and the inter-calibration methods are introduced. In section 3, we compare the inter-calibration results and analysis of FY-3B/MWRI and Aqua/AMSR-E

brightness temperature data. In section 4, the main results are summarized.

2. DATA SETS

The data sets include 8858 files of FY-3B/MWRI L1 and 9327 files of Aqua/AMSR-E L2A from November 18, 2010 to September 30, 2011. The spatial coverage of these data is north of 60°N. Data are downloaded from the NSMC (http://www.nsmc.cma.gov.cn/NSMC/Home/Index.html) and DAAC at NSIDC (http://nsidc.org/) respectively. The main technique and Instrument parameters setting of MWRI were basically consistent with those of AMSR-E on channel 10.7-89GHz. AMSR-E and MWRI are dual-polarized, the equatorial transit time is 1:30 and 1:40 and the incident angle is 55° and 53.5° respectively. In view of this, statistical inter-calibration approach is used to compare MWRI and AMSR-E brightness temperature directly.

3. INTER-CALIBRATION METHODS

The inter-calibration methods are divided into steps: (1) Radiometric calibration. Processing the sensors HDF strip files, extracting the longitude and latitude data, DN data, and scan line time from 10.7GHz to 89.0GHz channels. Converting the DN values to TB values, the radiometric calibration is applied as:

$$TB=S\times DN+I$$

where S=0.01, I=327.68, S is the scale factor, I is the offset. (2) Data quality control and time-spatial matching. Firstly, the horizontal and vertical gradient threshold method is used to remove the abnormal or error data. The data is removed if the gradient value more than 10 K. Secondly, based on the land mask with resolution of 12.5km×12.5km from NSIDC, select 7×7 window to expand the land mask, the data will be marked as invalid value if there exist land point in the window. Thirdly, project the MWRI and AMSR-E data from 10.7GHz to 89.0GHz to the research region by using spherical polar projection. The matching time window is no more than 30 minutes. Then the time-space matching data between the MWRI and AMSR-E is achieved. (3) Detect and remove sea-ice edges. Use the ratio of 18.7V and 36.5V of the AMSR-E TB, the intensity ratio and its gradient to determine the threshold of sea ice edges [14]. In the research data sets, the threshold of sea ice edge α_0 is obtained and it mainly range from 0.88 to 0.915 as shown in Fig,1. So select 0.9 as the sea ice edges threshold and 3×3 grid is further used as a template to remove the data that contain both sea ice and open water. (4) Inter-calibration based on linear fitting. According to the space-time matching matrix, the one-dimension sequence data set used for inter-calibration is obtained. Because of the similar configuration and nearly simultaneous satellite overpass times of the two radiometers, the linear fitting analysis based on the least square method is applied. The fitting linear function is shown in the formula:

$$TB'_{MWRI}=a\times TB_{MWRI}+b$$

where a and b represent the slope and intercept after linear fitting of the brightness temperature data between MWRI and AMSR-E, TB_{MWRI} is the TB data of MWRI, TB'_{MWRI} is the data obtained by the calibration fitting.

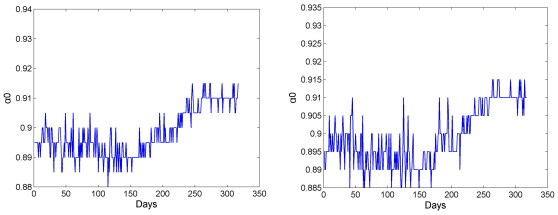

Ascending data Descending data

Fig.1. Time series of boundary ratio α_0

4. RESULTS AND ANALYSIS

4.1 Consistency of the MWRI and AMSR-E data

With the 10 channels TB data of the MWRI and AMSR-E, two thirds data are used as the calibration data, and one third as the test data. From December 1, 2010, the monthly data in the data set were taken as the time unit for statistical analysis and the matching points range, bias range and its mean, standard deviation range and its mean are shown in Tab.1 and Tab.2.

It can be seen from the bias that the TB data of MWRI is smaller than that of AMSR-E, except 18.7H and 36.5H. At the same frequency, the absolute bias and standard deviation of the V polarization are greater than those of the H polarization.

Table 1. Monthly statistics of TB difference between MWRI and AMSR-E (Ascending)

		10.7V	18.7V	23.8V	36.5V	89V
Number		2528869～2958829	2582360～2993550	2574811～2996416	2518217～2935038	1965602～2542164
bias/K	range	-8.8912～0.5443	-5.7055～1.3932	-6.7467～0.5500	-8.8760～1.9513	-3.4882～0.0953
	mean	-3.8866	-1.6455	-3.1829	-2.7182	-1.4080
Standard deviation/K	range	2.5949～4.5250	2.1969～3.6039	1.9472～3.2045	2.3755 ～4.1643	1.5258～3.9636
	mean	3.3409	2.9308	2.5595	3.1336	2.4629
		10.7H	18.7H	23.8H	36.5H	89H
Number		2299335～2838553	2351157～2874833	2235530～2801504	1949009～2570270	1118481～1741483
bias/K	range	-7.1920～3.2777	-2.0388～3.8471	-2.9265～3.0452	-2.0247～3.9863	-1.8203～1.0726
	mean	-1.0848	0.6743	-0.3437	0.6802	-0.3750
Standard deviation/K	range	2.1418～3.6613	1.5276～2.6593	1.5318～3.0101	1.6173～3.4798	1.7409～3.9029
	mean	2.5679	2.0753	2.2365	2.3223	2.5274

The range of the bias is -7.1920~3.9863K and -8.8912 ~1.9513K (ascending orbit), -5.7039~4.3616K and -8.8711 ~1.4231K (descending orbit) on H and V polarization respectively. The mean bias range of all the month is -1.0848~0.6802K and -3.8866~-1.4080K (ascending orbit), -0.0417~1.3047K and -3.9361~-1.0857K (descending orbit) on H/V polarization respectively. The standard deviation

range is 1.4363~4.3141K and 1.4564~4.5250K on H/V polarization respectively. Based on the transmitting mode of radiation on the ocean surface, the difference of incident angle and polarization mode will lead to the deviation of brightness temperature. There are some deviation between the MWRI and AMSR-E data but it has obvious consistency on overall trend.

Table 2. Monthly statistics of TB difference between MWRI and AMSR-E(Descending)

		10.7V	18.7V	23.8V	36.5V	89V
Number		1204820~2241922	1227449~2270212	1230016~2273302	1214670~2229946	1542418~2035397
bias/K	range	-8.8041~0.6433	-5.6051~1.4231	-6.5357~0.7525	-8.8711~1.3514	-2.6852~0.2463
	mean	-3.9361	-1.6453	-3.0567	-2.7856	-1.0857
Standard deviation/K	range	2.2687~4.5015	2.0272~3.6874	1.6942~3.3144	2.0325~4.2722	1.4564~3.6637
	mean	3.3330	2.8658	2.5459	3.0371	2.4067
		10.7H	18.7H	23.8H	36.5H	89H
Number		1145060~2149452	1169977~2178805	1129341~2116830	1013328~1924867	658719~1358748
bias/K	range	-5.7039~3.6198	-0.9728~3.9682	-2.4931~3.3122	-1.7688~4.3616	-1.2652~1.2547
	mean	-0.3637	1.2352	0.2309	1.3047	-0.0417
Standard deviation/K	range	1.9829~4.3141	1.4363~2.8994	1.5791~3.0979	1.6785~3.622	1.7611~4.0923
	mean	2.5672	2.0754	2.2907	2.3987	2.5866

4.2 Inter-calibration result analysis

In September, taking H polarization ascending calibration data as example, the scatters of each channel are obtained by regression analysis as shown in Fig. 2. It can be seen that there is a linear relationship between MWRI and AMSR-E. The slopes and the intercepts of the fitting equations list in the Tab.3. Based on the fitting equations, using the test data, the statistic parameters before fitting and after fitting were obtained by linear regression on each channel.

From Fig.2, it can be seen that the correlation coefficients of the two sensors TB are more than 0.99. The slopes and intercepts of the fitting equations are between 1.0004~1.0231 and -2.9216~0.3718K. The statistic parameters of the test data after inter-calibration such as RMSE, MAE, mean deviation(mean), were optimized significantly than those before the fitting.

Further, linear regression analysis was carried out on each channel in the data sets. The slopes and intercepts of the fitting equations on every month were obtained as shown in Tab.3 and 4. From the table, it shows that in H polarization the slope range of the inter-calibration of each channel is 0.9780~1.0392 and 0.9777~1.0369, both of which are close to 1, the intercept range is -7.2444~2.9007K and -6.6162~3.4304K on the ascending and descending data respectively. In the V polarization it shows that some slopes in 18.7 and 36.5GHz are less than 0.9. Except the 89GHz V polarization, most of the intercepts of the fitting results are larger than those of H polarization.

Except 89.0GHz, the slopes of each channel in horizontal polarization are close to 1. However, the slopes of other channels in vertical polarization are less than 1. The vertical polarization intercepts are larger than that of the horizontal polarization channels which distribute in 12.2824~44.1591K.

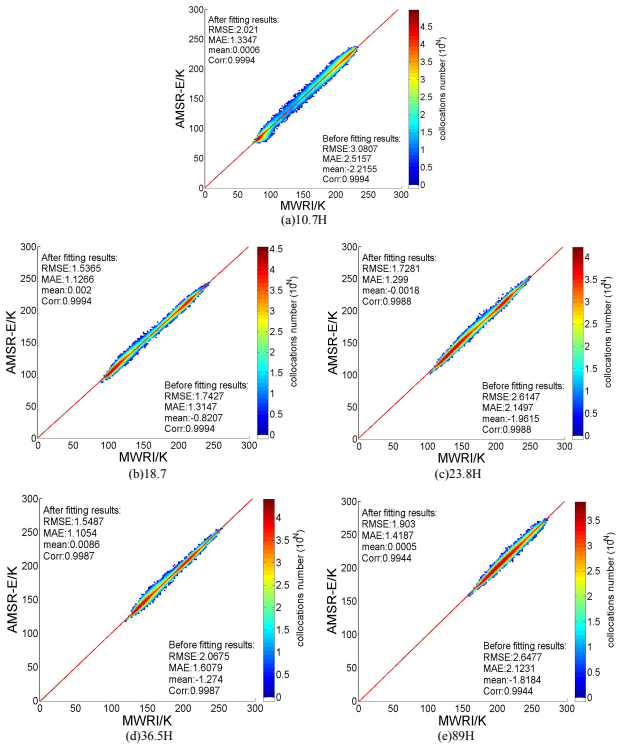

Fig.2. Inter-calibration results of the channel 10.7~89.0GHz, H polarization ascending data

Table 3. Slopes and intercepts (Ascending)

	10.7V		18.7V		23.8V		36.5V		89V	
	Slope	Intercept	Slope	Intercept	Slope	Intercept	Slope	Intercept	Slope	Intercept
2010/11	0.9527	14.9258	0.9509	12.2824	0.9540	15.4747	0.9078	20.0667	1.0128	-1.4098
2010/12	0.9430	15.5413	0.9444	12.4150	0.9272	19.7408	0.9033	20.5372	1.0485	-10.5969
2011/1	0.9094	19.7016	0.9036	20.6075	0.9060	20.9660	0.8746	28.1550	1.0009	-0.2244
2011/2	0.9103	19.6612	0.9023	21.0495	0.9037	21.6276	0.8667	30.0311	1.0048	-1.3512
2011/3	0.9126	19.6436	0.9068	20.3602	0.9118	20.1683	0.8778	27.8701	0.9964	0.5756
2011/4	0.9140	20.0176	0.9076	20.6961	0.9104	21.1461	0.8710	30.1646	1.0039	-0.7457
2011/5	0.9215	20.0619	0.9154	20.2926	0.9162	21.4443	0.8632	33.9434	0.9950	1.8612
2011/6	0.9418	18.9998	0.9256	20.0321	0.9290	21.2405	0.9101	27.0193	1.0107	-0.4781
2011/7	0.9446	18.6246	0.9260	20.2348	0.9283	21.9742	0.8861	33.2514	1.0007	1.9159
2011/8	0.9507	17.3995	0.9295	19.2642	0.9343	20.3250	0.8929	31.4947	0.9770	8.2201
2011/9	0.9448	17.9238	0.9171	20.9754	0.9134	23.7086	0.8477	40.1699	0.9995	2.8060
	10.7H		18.7H		23.8H		36.5H		89H	
	Slope	Intercept	Slope	Intercept	Slope	Intercept	Slope	Intercept	Slope	Intercept
2010/11	1.0241	2.6645	1.0255	-2.8410	1.0324	-3.4142	1.0392	-7.2444	1.0109	-1.6769
2010/12	1.0066	2.6345	1.0136	-2.6710	1.0155	-2.2463	1.0235	-5.7709	1.0125	-2.5811
2011/1	0.9780	0.5200	0.9784	0.2346	0.9831	0.0853	0.9887	-2.0166	0.9874	1.5406
2011/2	0.9795	0.4719	0.9790	0.2566	0.9834	0.1695	0.9884	-1.7647	0.9800	2.9007
2011/3	0.9814	0.5871	0.9806	0.2340	0.9876	-0.4022	0.9913	-2.0720	0.9895	1.0102
2011/4	0.9832	0.9101	0.9806	0.6292	0.9857	0.5025	0.9928	-1.8568	0.9922	0.8232
2011/5	0.9896	1.2056	0.9855	0.8787	0.9902	1.0234	0.9923	-0.4058	0.9920	1.4645
2011/6	1.0115	0.5094	1.0015	0.4254	1.0074	0.6657	1.0216	-2.2291	1.0095	-0.9263
2011/7	1.0198	-0.3379	1.0058	0.0849	1.0093	0.8232	1.0214	-2.1596	1.0109	-1.2824
2011/8	1.0214	-0.5572	1.0073	-0.2722	1.0139	-0.1293	1.0265	-3.0896	1.0142	-1.7573
2011/9	1.0134	-0.0902	1.0004	0.1354	1.0068	0.3718	1.0231	-2.9216	1.0181	-2.6222

Table 4. Slopes and intercepts (Descending)

	10.7V		18.7V		23.8V		36.5V		89V	
	Slope	Intercept	Slope	Intercept	Slope	Intercept	Slope	Intercept	Slope	Intercept
2010/11	0.9486	15.9961	0.9468	13.5497	0.9546	15.6272	0.9195	17.4291	1.0091	-0.0840
2010/12	0.9467	15.4129	0.9446	12.9171	0.9440	16.8656	0.9230	15.8538	1.0449	-9.3799
2011/1	0.9062	20.9331	0.8990	21.9430	0.9042	21.7066	0.8843	26.0297	1.0050	-1.2559
2011/2	0.9069	20.8843	0.8989	22.0450	0.9025	22.1868	0.8779	27.6490	1.0073	-1.6593
2011/3	0.9097	21.0616	0.9036	21.6011	0.9105	20.9341	0.8865	26.2256	1.0026	-0.2085
2011/4	0.9151	20.6768	0.9072	21.6194	0.9098	21.9065	0.8768	29.1632	1.0054	-0.6154
2011/5	0.9199	20.9721	0.9140	21.2147	0.9167	21.7655	0.8737	31.9643	0.9863	4.1702
2011/6	0.9389	19.8283	0.9245	20.6592	0.9280	21.8496	0.9010	29.7571	0.9945	3.4367
2011/7	0.9412	19.5281	0.9239	21.0170	0.9258	22.8339	0.8888	33.1197	0.9514	14.4421
2011/8	0.9449	18.9263	0.9232	21.0547	0.9260	22.5833	0.8894	32.6197	0.9774	8.5172
2011/9	0.9379	19.9525	0.9076	23.5032	0.8996	27.2242	0.8306	44.1591	1.0223	-1.8940
	10.7H		18.7H		23.8H		36.5H		89H	
	Slope	Intercept	Slope	Intercept	Slope	Intercept	Slope	Intercept	Slope	Intercept
2010/11	1.0229	3.3254	1.0259	-2.6621	1.0345	-3.5790	1.0369	-6.0963	1.0013	0.3598
2010/12	1.0182	2.2751	1.0227	-3.4251	1.0286	-3.7320	1.0340	-6.6162	1.0151	-2.9858
2011/1	0.9779	1.0445	0.9777	0.6061	0.9828	0.4828	0.9878	-1.4376	0.9894	1.1583
2011/2	0.9786	1.1630	0.9778	0.7900	0.9830	0.5754	0.9878	-1.1760	0.9789	3.4304
2011/3	0.9820	1.1885	0.9808	0.7271	0.9878	0.0802	0.9915	-1.4964	0.9925	1.0475
2011/4	0.9858	1.2006	0.9823	1.0716	0.9859	1.1120	0.9910	-0.9914	0.9896	1.9534
2011/5	0.9908	1.3010	0.9859	1.2817	0.9901	1.4539	0.9948	-0.6598	0.9918	1.8697
2011/6	1.0111	0.7064	1.0004	0.9292	1.0047	1.4814	1.0188	-1.7371	1.0042	0.2652
2011/7	1.0184	0.0288	1.0055	0.4742	1.0070	1.5581	1.0201	-1.7739	1.0012	1.0425
2011/8	1.0205	0.0042	1.0066	0.3201	1.0087	1.1496	1.0197	-1.7688	1.0073	0.0979
2011/9	1.0125	0.7676	0.9989	0.9706	1.0015	1.7253	1.0166	-1.3924	1.0166	-1.5714

5. CONCLUTIONS

In this paper, the inter-calibration of the TB between MWRI and AMSR-E is studied from November 18, 2010 to September 30, 2011 on Arctic. With the polar projection, time-space matching and linear fitting method, the inter-calibration parameters of the two sensors are achieved. The results show that the TB distribution of the two sensors are consistent and strong correlation. Compared with the bias and the standard deviation, the deviations of the H polarization data are relatively small. There are some deviation between the MWRI and AMSR-E TB data but it has obvious consistency on overall trend. The slopes and the intercepts are achieved using the data sets. After inter-calibration the performance parameters between MWRI and AMSR-E data are obviously optimized. Although the parameters of MWRI and AMSR-E are similar, there is a certain difference in the ground resolution and incident angle. In the future research, improvements will be made in this aspect to decrease the range of difference between the two sensors.

ACKNOWLEDGEMENTS

This work was supported by the Global Change Research Pr ogram of China (2015CB953901) and the National Key Research and Development Program of China (2016YFC1402704). MWRI were provided by the NSMC Satellite Data Center. AMSR-E were provided by DAAC of NASA at American National Snow and Ice Data Center .

REFERENCES

[1] Parkinson C L, Cavalieri D J., "Arctic sea ice variability and trends, 1979–2006," *Journal of Geophysical Research: Oceans (1978–2012)*, 113(C7), 2008.

[2] Spreen G, Kaleschke L and Heygste G, " sea ice remote sensing using AMSR-E 89GHz channels," *J. Geophys. Res*, 113(C2), DOI: 10.1029/2005JC003384, 2008.

[3] Kunzi K F, Patil S and Rott H., "Snow-cover parameters retrieved from Nimbus-7 scanning multichannel microwave radiometer (SMMR) data," *IEEE Transaction on Geoscience and Remote Sensing*, 20(4), pp.452–467, 1982.

[4] Hollinger J P, Peirce J L and Poe G A, "SSM/I instrument evaluation," *IEEE Transactions on Geoscience and Remote Sensing*, 28(5), pp.781-790, 1990.

[5] Comiso J C, Cavalieri D J and Markus T, "Sea ice concentration, ice temperature, and snow depth using AMSR-E data," *IEEE Trans. Geosci. Remote Sensing*, 41(2), pp.243-252, 2003.

[6] DAI Li-yun, CHE Tao, "An Calibration of passive Microwave Brightness temperature between SMMR and SSM/I," *Remote sensing technology and Application,* 24(5), pp.617-621, 2009.

[7]Okuyama A, Imaoka K., "Intercalibration of Advanced Microwave Scanning Radiometer-2 (AMSR2) Brightness Temperature," *IEEE Transactions on Geoscience & Remote Sensing*, 53(8), pp.4568-4577, 2015.

[8] Imaoka K. , Kachi M. , Kasahara M. , Ito N. , Nakagawa K. and Oki, T. , "Instrument performance and calibration Of AMSR-E and AMSR2," *International Archives of the Photogrammetry, Remote Sensing and Spatial Information Science,* 38(8), pp.13-16, 2010.

[9] Hu Tongxi, Zhao Tianjie, et al., "Inter-Calibration of AMSR-E and AMSR2 Brightness Temperature," *Remote Sensing Technology and Application*, 31(5)，pp. 919-924, 2016.

[10] Du J. , Kimball J.S. , Shi J. , et al., "Inter-Calibration of Satellite Passive Microwave Land Observations from AMSR-E and AMSR2 Using Overlapping FY3B-MWRI Sensor Measurements," *Remote Sens.*, 6(9), pp.8594-8616, 2014.

[11] Huang Wei, HAO Yan-Ling, WANG Jin et al., "Brightness Temperature Data Comparison and Evaluation of FY-3B MicroWave Radiation Imager with AMSR-E," *Periodical of Ocean University of China*, 43(11), pp.99～111, 2013.

[12] Wang Gongxue, Jiang Lingmei,Wu Shengli, et al., "Intercalibrating FY-3B and FY-3C/MWRI for Synergistic Implementing to Snow Depth Retrieval Alogorithm," *Remote Sensing Technology and Application*, 32(1), pp.49-56, 2017.

[13]Yang H, et al., "The FengYun-3 Microwave Radiation Imager On-Orbit Verification," *IEEE Transactions on Geoscience and Remote Sensing*, 49(11), pp.4552-4560, 2011.

[14]Zhang Shugang, "An Algorithm to Detect Arctic Sea Ice Edge Using Microwave Brightness Temperature," *Periodical of Ocean University of China*, 42(11), pp.1-7, 2012.